Classifiers and Confidence Estimation for Oil Spill Detection in ENVISAT ASAR Images

Camilla Brekke and Anne H. S. Solberg, *Member, IEEE*

***Abstract*—An improved classification approach is proposed for automatic oil spill detection in synthetic aperture radar images. The performance of statistical classifiers and support vector machines is compared. Regularized statistical classifiers prove to perform the best on this problem. To allow the user to tune the system with respect to the tradeoff between the number of true positive alarms and the number of false positives, an automatic confidence estimator has been developed. Combining the regularized classifier with confidence estimation leads to acceptable performance.**

***Index Terms*—Classification, oil spill, synthetic aperture radar (SAR).**

I. Introduction

OIL SPILLS appear as dark areas in synthetic aperture radar (SAR) images because the oil damps the short gravity waves on the sea surface. A part of the oil spill detection problem is to distinguish oil spills from other low-backscatter ocean phenomena (*look-alikes*) creating dark structures in the images. The framework of our algorithm is a dark spot detector, a feature extractor, and a dark spot classifier. Dark spots in the images are primarily detected by adaptive thresholding. For each of them, a number of features are computed to classify the slick as either an oil spill or a look-alike. Segmentation and feature selection were discussed in [1] and [12]. In this paper we focus on the classification step.

Various classifiers have been applied to the oil spill detection problem. A Mahalanobis classifier and a compound probability classifier were applied in [5]. The probabilistic approach was improved in [9] by using a different classification algorithm including a multiregression approach where the regression coefficients represent the contribution of each feature on the prediction of a new sample. A neural-network approach is described in [6], and in [7], a classifier based on fuzzy logic is presented. In [8], a support vector machine (SVM) technique for oil spill detection was applied.

Oil spill detection is an application where the classifier should detect a rare but important event (look-alikes appear much more frequent). Based on a statistical classifier for oil spill detection described earlier [12], we here suggest the introduction of regularization of the covariance matrices to decrease the number of false positives. SVM has been used for a number of applications often showing good performance [2]. We compare SVM to the regularized statistical classifier. Confidence levels automatically assigned to the slicks can be useful for prioritizing the alarms and helpful as a "second opinion" to manual analysis [11]. We present a novel algorithm for automatic assignment of confidence levels.

Manuscript received June 19, 2007.

C. Brekke is with the Norwegian Defence Research Establishment, 2027 Kjeller, Norway, and also with the Department of Informatics, University of Oslo, 0316 Oslo, Norway (e-mail:camilla.brekke@ffi.no).

A. H. S. Solberg is with the Department of Informatics, University of Oslo, 0316 Oslo, Norway.

Digital Object Identifier 10.1109/LGRS.2007.907174

II. SAR Images

Our system is trained and tested on 103 complete ENVISAT ASAR Wide Swath Mode images. The image set is split into three sets: training (56 images), validation (20 images), and testing (27 images). The images are collected from the Baltic Sea and the North Sea from 2003 to 2005. Aircraft verifications from a joint airborne-satellite campaign [10] are available for the test set. To label the training and validation sets, oil slick candidates were manually masked and associated with the "high confidence" and "moderate confidence" categories (this information was used in the training of the confidence estimator, Section III-C). For more details on the masking process, see [12].

III. Classification Methodology

For each of the segmented dark spots i, a number of features (selected in previous studies [1], [13]) are computed: shape features—"sum of external angles," "slick moment (MOM)," "slick area," "slick complexity," and "slick width"; contrast features—"slick local contrast," "slick border," and "smoothness contrast"; texture—"power-to-mean ratio (PMR)" and "slick variance"; and surroundings—"regions in small neighborhood" and "distance to ship/oilrig." In addition, a new feature "low wind area" is developed. It is defined as a binary feature, which is assigned 1 if the region overlaps with a large region ($\geq$ 4000 pixels, i.e., larger than the largest oil spill observation among the training samples) in a coarse segmented version of the image where large dark structures at the size of large low wind areas will be detected.

The simplest classifier to consider is to use a multivariate Gaussian classifier. However, the behavior of the features will change with different wind levels. Describing the conditional density by a unimodal density such as a Gaussian is, therefore, not appropriate. If we split the problem and assume different densities depending on the wind level, we can train a classifier for each subclass. The data within each subdivision would then be reasonably homogeneous, and it might be appropriate to assume the densities to be Gaussian.

The class-conditional multivariate normal density is completely specified by $d + d(d+1)/2$ parameters, namely the elements of the class-specific mean vector μ_k and the independent elements of the covariance matrix Σ_k. d is the

dimensionality of the feature vector. As oil spills just occasionally occur, we need to consider robust estimation of Σ_k due to the low number of training samples. We suggest regularization of the estimated covariance matrix by forming a combination of the fully estimated covariance matrix and the diagonal covariance matrix.

Oil spill detection based on SAR is today used in combination with surveillance aircraft in many European countries. In addition to the cost of sending out an aircraft, the false alarm ratio acceptable by the customers could vary. It would be desirable that the automatic system not only reports which slicks were classified as oil but also the probability associated with that decision. Using the computed posterior probability for this purpose would be the first option to consider. However, initial experiments indicated that this did not perform well. The posterior probability for a two-class Gaussian tends to be very close to either 1 or 0. Comparing the probabilities across subclasses also turned out to be difficult because of the difference in variance between the subclasses. To reduce the number of false positives and to give the operator a tool for prioritizing the alarms, we have developed an automatic confidence estimator for all spots labeled oil spill by the classifier. First, a classifier is applied to each feature vector $\mathbf{x}_i$, then for each slick with a higher posterior probability of being an oil spill than a look-alike ($\Pr(\text{oil spill}|\mathbf{x}_i) > \Pr(\text{look-alike}|\mathbf{x}_i)$) a confidence level is automatically estimated.

A. Statistical Classifier

In [12] and [13], a prior distribution and a probability density for the features are combined through Bayes' theorem to obtain the *posterior* probability for a detected spot being an oil spill. Let c be the unknown class membership of a detected spot (we are dealing with a two-class problem: oil spill or look-alike). Then

$$\Pr(c = o|\mathbf{x}_i) = \frac{\pi_o f_o(\mathbf{x}_i)}{\pi_o f_o(\mathbf{x}_i) + (1-\pi_o) f_l(\mathbf{x}_i)} \tag{1}$$

where π_o is the prior model for the probability that a detected spot is oil. $f_o(\mathbf{x}_i)$ and $f_l(\mathbf{x}_i)$ are the probability densities for the observed features $\mathbf{x}_i$ in classes $o =$ oil spills and $l =$ look-alikes, respectively. The densities are assumed Gaussian, i.e.,

$$f_c(\mathbf{x}_i) = \frac{1}{(2\pi)^{\frac{d}{2}}|\Sigma|^{\frac{1}{2}}} \times \exp\left\{-\frac{1}{2}(\mathbf{x}_i - \mu_c)^T \Sigma^{-1}(\mathbf{x}_i - \mu_c)\right\} \tag{2}$$

where $c \in \{o, l\}$, d is the number of features, μ_c is the mean vector for class c, and Σ is the covariance matrix, common for both classes due to the imbalanced data set. Only "slick complexity," "PMR," "slick local contrast," "slick width," "regions in small neighborhood," "slick border," "smoothness contrast," and "slick variance" are included in feature vector $\mathbf{x}_i$.

1) Division of Each Class Into a Set of Subclasses: Even within each wind level W, both the oil slicks and the look-alikes may vary quite a lot in shape, contrast, and other features. The wind level W is first used to divide the samples in two different subclasses and then these are divided into five subclasses based on the shape descriptor "MOM" (see Table I). The wind level is represented by a homogeneity category $\in \{1, \ldots, 6\}$ estimated based on the "PMR" of the surroundings [12]. The division of the feature space might not be optimal and is the subject of ongoing research.

TABLE I
SUBCLASSES AND THE NUMBER OF OBSERVATIONS IN THE TRAINING SET

Subclass	MOM	PMR	Oil Spills	Look-alikes
1	$<$ 0.3	$>$=0.04	37	5267
2	$\in [0.3, 0.5)$	$>$=0.04	34	4202
3	$\in [0.5, 0.8)$	$>$=0.04	23	1681
4	$\in [0.8, 1.2)$	$>$=0.04	12	617
5	$>$=1.2	$>$=0.04	16	278
6	$<$0.3	$<$ 0.04	23	786
7	$\in [0.3, 0.5)$	$<$ 0.04	25	604
8	$\in [0.5, 0.8)$	$<$ 0.04	14	152
9	$\in [0.8, 1.2)$	$<$ 0.04	9	51
10	$>$=1.2	$<$ 0.04	14	27

2) Covariance Matrix Estimation: With the subclass division, the density for class c and wind level W is then given by $f_{c,W,g}(\mathbf{x}_i)$ if "MOM" is in shape subgroup g. Different densities depending on the value of "MOM" are assumed. Applying Gaussian densities, the simplest classifier consists of using common diagonal covariance matrices for each subclass: $\hat{\Sigma}_{W,g} = \text{diag}\{\Sigma_{W,g}\}$, where $\Sigma_{W,g}$ is the fully estimated common covariance matrix. Replacing $\hat{\Sigma}_{W,g}$ with a regularized covariance matrix leads to a more general family of covariances indexed by $\rho_{W,g}$, i.e.,

$$\widetilde{\Sigma}_{W,g}(\rho_{W,g}) = \rho_{W,g}\left[\text{diag}\{\Sigma_{W,g}\}\right] + (1-\rho_{W,g})\Sigma_{W,g}. \tag{3}$$

Here, $\rho_{W,g} \in [0, 1]$ allows a continuum of models and needs to be specified through experiments. If class-dependent covariance matrices are used, the variance of the look-alike class could be huge compared to the oil class, and the resulting class-conditional probabilities for the look-alikes would be of another magnitude than for oil resulting in a large "bias" in the classification. A way of handling the very unbalanced data set is to avoid using class-conditional covariance matrices. However, how imbalanced the training set varies among the subclasses. If we use class-conditional covariance matrices within each subclass, regularization can be expressed as

$$\widetilde{\Sigma}_{c,W,g}(\rho_{W,g}) = \rho_{W,g}\left[\text{diag}\{\Sigma_{c,W,g}\}\right] + (1-\rho_{W,g})\Sigma_{c,W,g} \tag{4}$$

where $c \in \{o, l\}$, and $\Sigma_{c,W,g}$ is the fully estimated class-conditional covariance matrix.

3) Loss Functions and Prior Probabilities: We are considering the misclassification of oil spills as look-alikes more serious than the misclassification of look-alikes as oil spills. A spot is classified as oil if

$$\frac{f_l(\mathbf{x}_i)}{f_o(\mathbf{x}_i)} < \frac{\pi_o l_1}{(1-\pi_o) l_2}. \tag{5}$$

Equal prior probabilities for the oil spill and the look-alike classes ($\pi_o = \pi_l = 0.5$) are applied, and $l_1 = \beta 0.6$ and $l_2 = 0.4$. $\pi_o = 0.5$ is far from realistic, as an oil spill is considered a rare event compared to look-alikes; however, π_o is adjusted in (5) through β which is based on a model presented in [12] and [13] for the expected number of look-alikes and oil spills

TABLE II
OPTIMAL SELECTION OF $\widetilde{\Sigma}$ AND ρ FOR EACH SUBCLASS

Subclass	ρ	$\widetilde{\Sigma}$
1	0	common
2	0	common
3	0.1	common
4	0	class-conditional
5	0	class-conditional
6	0.1	common
7	0	common
8	0.1	common
9	0.8	common
10	1	common

TABLE III
OPTIMAL SELECTION OF C, γ, w_1, AND w_{-1} FOR C-SVC

Subclass	$\gamma[2^x]$	$C[2^x]$	w_1	w_{-1}
1	-15.25	16.75	142	1
2	-8	15.5	123	1
3	-2.75	-4.25	73	1
4	-2	12	51	1
5	2.5	-3	17	1
6	-0.75	-5.75	33.5	1
7	-3.5	-6	23.5	1
8	-0.25	-4.25	10.5	1
9	-3.5	-2.25	5.2	1
10	-1.5	1	1.9	1

depending on the wind level. In total, this gives a reasonably realistic model for the imbalanced class problem.

4) Training the Regularized Classifier: A search for the optimal regularization parameter ρ and experiments to compare regularization with common versus class-conditional covariance matrices have been done. As some of the subclasses have a quite limited number of training samples, we chose to use cross validation with *leave-one-out* on the training set to identify optimal values for ρ within each subclass. The validation set was used to compare the performance of (3) and (4). The result is presented in Table II. To study the effect of regularization on the classifier (Section IV), two versions of the statistical classifier were trained: a classifier applying common diagonal covariance matrices, as in [12], and a regularized classifier. Our regularization technique adapts to the subclasses and is likely to generalize better than diagonal covariance matrices. For the small subclasses 9 and 10, the optimal ρ was found to be close to 1 (giving diagonal covariance matrices). The results also showed that, for subclasses 1–8 (a majority of the subclasses), the optimal ρ is close to 0 which means that the classifier performs best using a nondiagonal covariance matrix. We found that class-conditional (compared to common) covariance matrices give a better result on the validation set only for subclasses 4 and 5 (which are the two least imbalanced subclasses among those with highest PMR).

B. SVMs

As the training set is imbalanced, we have chosen to use C-Support Vector Classification (C-SVC) for the special case where different penalty parameters are used for the oil spill and look-alike classes. We have applied an implementation by Chang and Lin [3]. In regular C-SVC [4], a common penalty parameter C is applied for both the classes.

Given a training set of feature vector—label pairs $(\mathbf{x}_i, y_i)$, $i = 1, 2, \ldots, N$, where $\mathbf{x}_i \in R^n$, and $y_i \in \{1, -1\}$ (note that, here, we are dealing with a two-class approach since we are considering a pair of classes, oil spill or look-alike), C-SVC requires training that involves the minimization of the error function, i.e.,

$$\min_{\mathbf{w},b,\xi} \frac{1}{2}\mathbf{w}^T\mathbf{w} + C_1 \sum_{y_i=1} \xi_i + C_{-1} \sum_{y_i=-1} \xi_i \qquad (6)$$

subject to

$$y_i \left(\mathbf{w}^T \phi(\mathbf{x}_i) + b\right) >= 1 - \xi_i, \qquad \xi_i >= 0, \quad i = 1, \ldots, N$$

where the ξ_i are slack variables which measure the degree of misclassification of $\mathbf{x}_i$, and $C_1 > 0$ is the oil spill and $C_{-1} > 0$ is the look-alike penalty parameters of the error terms, $\boldsymbol{w}$ is the vector of coefficients, and b is a constant. The feature vectors are mapped into a higher dimensional space by the kernel ϕ. A radial basis kernel function is used: $K(\mathbf{x}_i, \mathbf{x}_j) = \exp(-\gamma \|\mathbf{x}_i - \mathbf{x}_j\|^2)$, where $\gamma > 0$ is the kernel parameter to be specified. The same feature vector, as applied for the statistical classifiers, was applied here.

1) Training the C-SVC: In early attempts on applying regular C-SVC, almost all slicks were classified as look-alikes. Since we are dealing with an imbalanced data set, we added a cost model that makes errors on the oil spill examples more expensive. This improved the results. It is emphasized in (6) how the class-dependent penalty parameters C_1 and C_{-1} are applied in C-SVC. The penalty parameter for the oil spill class C_1 is set equal to $w_1 * C$, where w_1 is a weight. The penalty parameter for the look-alike class C_{-1} is set equal to $w_{-1} * C$, where w_{-1} is another weight. We selected $w_1 =$ number of look-alikes in subclass/number of oil spills in subclass and $w_{-1} = 1$. A standard *grid search* was done where pairs of (C, γ) were tried out, and the one with the best performance accuracy (on the validation set) was picked. The exponentially growing sequences $C = 2^{-5}, 2^{-4}, \ldots, 2^{15}$ and $\gamma = 2^{-15}, 2^{-14}, \ldots, 2^3$ were used for a coarse grid search. Then, a region on the grid containing the best validation accuracy was selected for a grid search with finer resolution. The final selection of C, γ, w_1, and w_{-1} used in the training of the classifier is presented in Table III. Each attribute of the feature vectors was scaled to the range $[-1, 1]$, as commonly done for SVM.

C. Automatic Confidence Estimation

A study performed by Solberg *et al.* in the Oceanides project [10] showed that a confidence manually assigned by the operator would be of high value to the surveillance aircraft if it is reliable. However, experiments involving several operators and aircraft detections showed that reliable and consistent assignment of confidence levels is difficult, and the manual procedure was subjective. We have thus developed an automatic (and objective) confidence estimator as a second step in our two-step classification approach. A confidence level is estimated for all slicks classified as oil spills in the first step of the classification approach.

To determine the confidence level of a slick, the operators at Kongsberg Satellite Services (KSAT) use a set of guidelines [10]. Early experiments showed that it is not sufficient to base the design of an automatic procedure only on these guidelines [11]. In addition to translating several of the KSAT criteria into computed features, we included additional features that we found important for reliable confidence estimation. An example is the KSAT guidelines for *High* confidence: "The slick has a large contrast to gray-level surroundings. The surroundings are homogenous, with a constant gray-level. The wind speed is moderate to high, i.e., approximately 6–10 m/s. Ship or platform directly connected to slick.", and the following rule established in our automatic confidence estimator: IF "slick local contrast" ≥ 0.91 AND "distance to ship/oilrig" ≤ 85.84 AND "PMR" ≤ 0.04 AND "regions in small neighborhood" ≤ 6 AND "MOM" ≥ 0.25 AND "slick area" ≥ 20 THEN HIGH (the feature limits are automatically estimated).

We use four confidence levels: *High, Medium, Low, and Very Low*. The following features for *High* are: "slick local contrast," "PMR," "regions in small neighborhood," "distance to ship/oilrig," "MOM," and "slick area." The following features for *Medium* are: "slick local contrast," "slick border," "sum of external angles," "PMR," "slick area," "regions in small neighborhood," and "low wind area." The following features for *Low* are: "low wind area," "PMR," "regions in small neighborhood," "sum of external angles," "slick border," "distance to ship/oilrig," "slick local contrast," "slick area," "smoothness contrast," and "wind."

Both the training and the validation sets were used in the training of the confidence estimator. The conditions for level *High and Medium* confidence were semiautomatically trained, whereas level *Low* was manually trained. For *High*, the feature value limits were automatically estimated from the computed feature vectors of the oil slicks. Depending on the feature, the limit was set at either the first or the last quartile of all the sorted feature values. We only applied those slick candidates in the training and the validation set that were marked "high confidence". The limit for the feature "PMR" was, however, slightly adjusted, as the automatic estimate appeared to be too strict. Confidence level *Medium* was trained in a similar manner as *High*, but here, we applied the first or the last quartile of *all* the feature vectors masked as oil spills in both the training and the validation sets for the initial estimation of the limits. Some of the limits were then manually adjusted after inspection of their performance on the validation set. The manual training of *Low* was basically done by visually studying the slicks in the validation images and their computed feature values.

IV. Comparing the Classifiers Performance

Table IV presents the performance accuracy on the test set for both the previously published statistical classifier and the new regularized statistical classifier. If we compare the classifier with common diagonal covariance matrices with the regularized one, there are 623 less false alarms after the regularization technique has been introduced. If we have a look at the oil spill class, we can see that we lose 5 out of 41 oil spills with the earlier published version of the classifier, whereas we only lose 3 out of 41 with the regularized one. Binary C-SVC for imbalanced data sets was evaluated against the regularized statistical classifier. It is clear from Table IV that C-SVC performs worse than the statistical classifiers for both the oil spill and the look-alike classes. Based on this, no further investigations with C-SVC were done.

TABLE IV
Classification Results on the Test Set

Classifier with Common Diagonal Covariance Matrices		
	Classified as Oil	Classified as look-alike
Marked as Oil	36 (87.8%)	5 (12.2%)
Marked as Look-alike	1879 (15.3%)	10366 (84.7%)
Classifier with Regularized Covariance Matrices		
	Classified as Oil	Classified as look-alike
Marked as Oil	38 (92.7%)	3 (7.3%)
Marked as Look-alike	1256 (10.3%)	10989 (89.7%)
C-SVC		
	Classified as Oil	Classified as look-alike
Marked as Oil	34 (82.9%)	7 (17.1%)
Marked as Look-alike	2768 (22.6%)	9476 (77.4%)

TABLE V
Performance Results for the Two-Step Classification Approach

High		
	Classified as Oil	Classified as Look-alike
Marked as Oil	13 (31.7%)	28 (68.3%)
Marked as Look-alike	8 (0.1%)	12237 (99.9%)
Medium (includes all High and Medium slicks)		
	Classified as Oil	Classified as Look-alike
Marked as Oil	21 (51.2%)	20 (48.8%)
Marked as Look-alike	30 (0.2%)	12215 (99.8%)
Low (includes all High, Medium and Low slicks)		
	Classified as Oil	Classified as Look-alike
Marked as Oil	32 (78.0%)	9 (22.0%)
Marked as Look-alike	94 (0.8%)	12151 (99.2%)
Very Low (includes all High, Medium, Low and Very Low slicks)		
	Classified as Oil	Classified as Look-alike
Marked as Oil	38 (92.7%)	3 (7.3%)
Marked as Look-alike	1200 (9.8%)	11045 (90.2%)

V. Confidence Estimation

Based on the results presented in Section IV, we selected the regularized statistical classifier for the first step of our classification approach. Each slick with a higher posterior probability of being an oil spill than a look-alike is then automatically assigned a confidence level. Table V summarizes the final classification accuracy. Here, the classifier was trained on 76 images (both the training and the validation set), compared to 56 in Table IV, which reduces the number of false alarms to 1200 for *Very Low* confidence level.

The trend found is that the surroundings of the detected slicks get more and more inhomogeneous and the number of look-alikes present increases for lower confidence levels. Fig. 1 presents some examples from the test set.

Counting the actual number of alarms, there were twice as many true positive as false positive alarms for the confidence category *High*, about an equal amount of true positive alarms and false positive alarms for *Medium*, and about half as many true positives as false positives for *Low*. The number of correctly recognized positive examples can, thus, be increased at

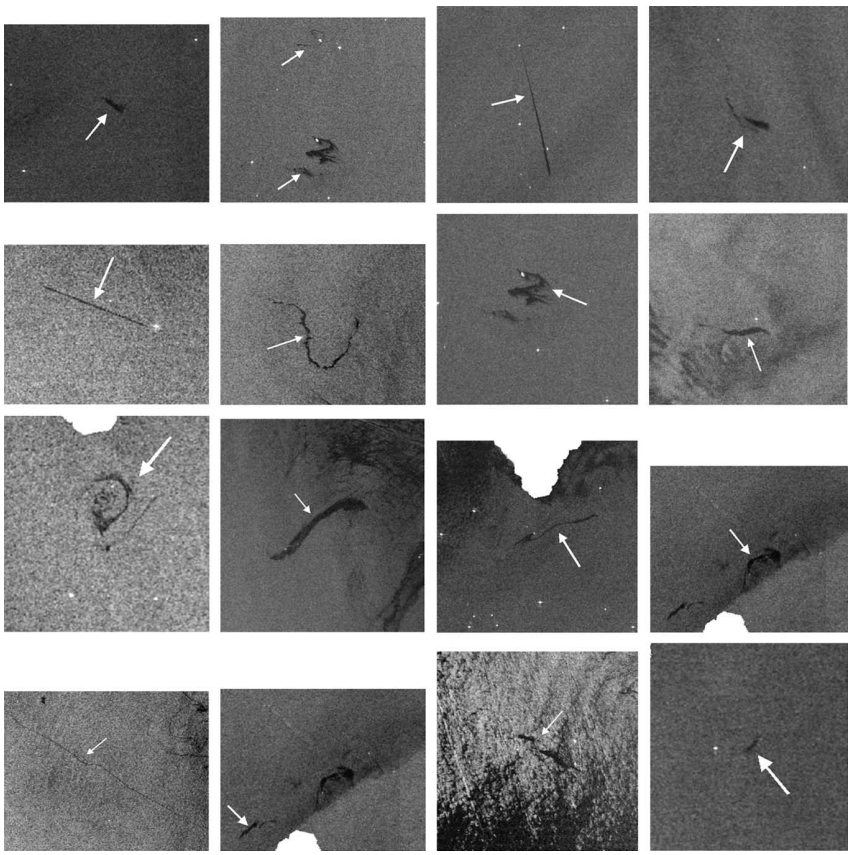

Fig. 1. Slicks automatically assigned as (first row) *High*, (second row) *Medium*, (third row) *Low*, and (fourth row) *Very Low* confidence. Note that as the confidence decreases, the surroundings of the slicks get more and more heterogeneous.

the cost of an increased number of false alarms, or vice versa. We believe that, for practical use, the *Low* confidence level would probably be the most suitable in most cases. The system is thus designed to produce some false alarms, which should be sorted out by manual inspection.

VI. Conclusion

We propose a two-step classification procedure for oil spill detection in SAR images, consisting of a regularized statistical classifier and an automatic confidence estimation of the detected slicks. This combination leads to an acceptable classification performance if the algorithm is run prior to a manual verification step before sending out aircraft/vessel. The performance is comparable to the results presented in [12], where a large rule base was trained to reduce the false alarm ratio. However, the approach proposed here is much easier to train as it is semiautomatically done, and the number of parameters to be adjusted is largely reduced. Compared to the classifier earlier proposed, the results presented here show that it is possible to largely reduce the false alarm ratio by introducing the regularization of the covariance matrices. By selecting a confidence level, the user is also able to tune the system with respect to the frequency of true positives versus false positives. The associated confidence level seems to be well correlated with the homogeneity of the surroundings. Information about algal blooms and wind is planned incorporated in future versions of the algorithm.

References

[1] C. Brekke and A. H. S. Solberg, "Segmentation and feature extraction for oil spill detection in ENVISAT ASAR images," *Int. J. Remote Sens.*, 2006. Submitted for publication.

[2] C. J. C. Burges, "A tutorial on support vector machines for pattern recognition," *Data Mining Knowl. Discov.*, vol. 2, no. 2, pp. 121–167, Jun. 1998.

[3] C.-C. Chang and C.-J. Lin, *LIBSVM: A Library for Support Vector Machines*, 2001. [Online]. Available: http://www.csie.ntu.edu.tw/~cjlin/libsvm

[4] C. Cortes and V. Vapnik, "Support-vector networks," *Mach. Learn.*, vol. 20, no. 3, pp. 273–297, Sep. 1995.

[5] B. Fiscella *et al.*, "Oil spill detection using marine SAR images," *Int. J. Remote Sens.*, vol. 21, no. 18, pp. 3561–3566, 2000.

[6] F. Del Frate *et al.*, "Neural networks for oil spill detection using ERS-SAR data," *IEEE Trans. Geosci. Remote Sens.*, vol. 38, no. 5, pp. 2282–2287, Sep. 2000.

[7] I. Keramitsoglou *et al.*, "Automatic identification of oil spills on satellite images," *Environ. Model. Softw.*, vol. 21, no. 5, pp. 640–652, May 2006.

[8] G. Mercier and F. Girard-Ardhuin, "Partially supervised oil-slick detection by SAR imagery using kernel expansion," *IEEE Trans. Geosci. Remote Sens.*, vol. 44, no. 10, pp. 2839–2846, Oct. 2006.

[9] F. Nirchio *et al.*, "Automatic detection of oil spills from SAR images," *Int. J. Remote Sens.*, vol. 26, no. 6, pp. 1157–1174, 2005.

[10] A. Solberg, P. Clayton, and M. Indregard. (2005, May). D2-Report on benchmarking oil spill recognition approaches and best practice. European Commission. [Online]. Available: http://oceanides.jrc.it/Arch. 04-10225-A-Doc; Issue 2.1, Contract No: EVK2-CT-2003-00177.

[11] A. H. S. Solberg, "Automatic oil spill detection and confidence estimation," in *Proc. Int. Symp. Remote Sens. Environ.*. St. Petersburg, Russia, 2005, pp. 943–945.

[12] A. H. S. Solberg *et al.*, "Oil spill detection in Radarsat and Envisat SAR images," *IEEE Trans. Geosci. Remote Sens.*, vol. 45, no. 3, pp. 746–755, Mar. 2007.

[13] A. H. S. Solberg *et al.*, "Automatic detection of oil spills in ERS SAR images," *IEEE Trans. Geosci. Remote Sens.*, vol. 37, no. 4, pp. 1916–1924, Jul. 1999.